PROCEEDINGS OF SPIE

SPIEDigitalLibrary.org/conference-proceedings-of-spie

Unidirectional response in spin-torque driven magnetization dynamics

J. Sklenar, W. Zhang, M. B. Jungfleisch, A. Hoffmann

J. Sklenar, W. Zhang, M. B. Jungfleisch, A. Hoffmann, "Unidirectional response in spin-torque driven magnetization dynamics," Proc. SPIE 10732, Spintronics XI, 1073212 (20 September 2018); doi: 10.1117/12.2321259

SPIE.

Event: SPIE Nanoscience + Engineering, 2018, San Diego, California, United States

Invited Paper

Unidirectional response in spin-torque driven magnetization dynamics

J. Sklenar[1], W. Zhang[2,4], M. B. Jungfleisch[3,4], A. Hoffmann[4]
[1]Department of Physics, University of Illinois at Urbana-Champaign, Urbana, IL 61801, USA; [2]Department of Physics, Oakland University, Rochester MI 48309, USA; [3]Department of Physics and Astronomy, University of Delaware, Newark, DE 19716, USA; [4]Materials Science Division, Argonne National Laboratory, Lemont IL 60439, USA

ABSTRACT

It was recently demonstrated in bilayers of permalloy and platinum, that by combining spin torques arising from the spin Hall effect with Oersted field-like torques, magnetization dynamics can be induced with a directional preference.[1] This "unidirectional" magnetization dynamic effect is made possible by exploiting the different even and odd symmetry that damping-like and field-like torques respectively have when magnetization is reversed. The experimental method used to demonstrate this effect was the spin-torque ferromagnetic (ST-FMR) resonance technique; a popular tool used in the phenomenological quantification of a myriad of damping-like and field-like torques. In this report, we review the phenomenology which is used to describe and analyze the unidirectional magnetization dynamic effect in ST-FMR measurements. We will focus on how the asymmetry in the dynamics also is present in the phase angle of the magnetization precession. We conclude by demonstrating a utility of this directional effect; we will outline an improved experimental method that can be used to distinguish a phase-shifted field-like torque in a ST-FMR experiment from a combination of field-like and damping-like torques.

1. INTRODUCTION

The spin-torque ferromagnetic resonance (ST-FMR) experimental technique[2] has risen in prominence because it has great flexibility in characterizing the growing database of spin-torque materials. In this work, we discuss a common realization of a ST-FMR measurement that is used to study spin-transfer torques (STT) in thin film heterostructures. Probably, the most common heterostructure studied is a bilayer consisting of a normal metal (NM) layer on top or below a ferromagnetic metal (FM) layer. We will refer to these bilayers as NM/FM samples, but as already indicated, the NM layer actually can be replaced by a wide range of materials. In earlier investigations, the NM layer was chosen to be a spin Hall metal[3] such as Pt,[2,4] Ta,[5] and W;[6,7] ST-FMR was then used to quantify spin Hall angles for these materials. Since then, a variety of other materials have been used in the place of spin Hall NM layers. Notable examples are antiferromagnetic metals,[8–10] topological insulators,[11] Rashba interfaces,[12] and two-dimensional materials;[13–15] all of these materials have been shown to produce significant damping-like STTs on an adjacent FM. Further proliferation of the ST-FMR method has led to alterations of the FM layer. It was predicted that ST-FMR could be observed in low-damping magnetic insulators with spin Hall metals,[16,17] and this effect has been observed.[18–22] Additionally, in patterned and nanostructured FM layers, a wide variety of resonant modes can be excited with ST-FMR.[23]

While ST-FMR has mainly thrived as an experimental technique to characterize damping-like (DL) and field-like (FL) torques, we have demonstrated that ST-FMR can also be used as an experimental platform to study directional effects in the response of high frequency magnetization dynamics.[1] Often, in thin film heterostructures one thinks of unidirectional effects as being germane to dc magnetoresistive properties. Indeed, FM/NM bilayers have been found to have intrinsic unidirectional magnetoresistance effects[24,25] that are related to spin valve physics. Our work, however, was an example of a new direction in the field of spintronics, where heterostructures are designed to promote a directional response in the magnetization dynamics. There are other examples of this trend in the literature, for instance, in permalloy/platinum[26,27]

Spintronics XI, edited by Henri-Jean Drouhin, Jean-Eric Wegrowe, Manijeh Razeghi, Henri Jaffès, Proc. of SPIE Vol. 10732, 1073212 · © 2018 SPIE
CCC code: 0277-786X/18/$18 · doi: 10.1117/12.2321259

and in magnetically-doped and non-magnetically-doped topological insulating bilayers,[28] unidirectional resistance asymmetries have been discovered when there is a dc current bias in the bilayer. In these situations, an asymmetry arises in the magnetoresistance which corresponds to whether or not the current bias excites or dampens magnons in the magnetic layer. Other examples of directional effects in magnetization dynamics can be found in system with the Dzyaloshinskii-Moriya interaction, which contributes a linear term in spin wave (magnon) dispersion relationships.[29,30]

Our specific contribution in this area of unidirectional magnetization dynamics, was to realize that the even and odd symmetry of DL and FL torques, under magnetization reversal, can be combined to create an asymmetric response in how magnetization precesses.[1] We demonstrated this in the well studied NM/FM system of permalloy/platinum. We found that in order for unidirectional dynamics to be excited, the magnetization of the system would have to be appreciably canted out of the plane of the sample. For these oblique magnetization orientations, ST-FMR can more efficiently be excited in one orientation with respect to a field-magnetization reversed counterpart.

In this report, we first summarize the unidirectional magnetization dynamic effect. We then examine an additional aspect of this effect which is related to asymmetries in the phase angle of the magnetization precession when the system is placed in a configuration which is promoting unidirectional dynamics. We will then discuss how the unidirectional effect can solve an issue which is sometimes present in ST-FMR measurements. Specifically, unidirectional dynamics can be used to rule out situations where phase shifts between the charge current passing through the device and the FL torques are falsely identified as DL spin-transfer torques.[31] This is a known experimental issue, but one which does not receive enough attention throughout the literature. By performing a measurement which promotes unidirectional dynamics, one can distinguish these two scenarios and, in principle, quantify the phase shift between the driving current and the FL torque.

2. THE ST-FMR EXPERIMENTAL METHOD AND UNIDIRECTIONAL MAGNETIZATION DYNAMICS

As illustrated in Figure 1 (a), a common ST-FMR measurement involves NM/FM bilayer samples directly integrated into a shorted, co-planar waveguide (CPW) geometry. By employing a bias-tee, a rf current is directly passed through the bilayer, and a dc voltage can be simultaneously measured across the sample when under resonance. The rf current passing through the bilayer can generate an oscillating FL torque on the FM layer which is illustrated by the red arrows which encircle the bilayer in Figure 1 (b). Additionally, a DL torque can be generated on the FM from a current passing through the NM layer. For illustrative purposes, we shall assume that the NM layer is Pt, and the DL torque is then generated from a bulk spin Hall effect. In our picture, the spin current generated by the spin Hall effect is illustrated with the yellow arrows; the spin current flows normal to the plane from the NM to the FM, and it is polarized in-plane and perpendicular to the charge current.

With the qualitative picture of the driving torques established, we now discuss the experimental method in more detail. Typically, a high frequency signal generator is fixed at a frequency ω [as shown in the circuit of Figure 1 (a)] and an external field is applied at some angle relative to the current and the field is swept. As indicated in Figure 1 (c), the external field is described by an in-plane azimuthal angle ϕ and a polar angle θ. The FM layers used in experiments are usually low-damping materials such as permalloy and YIG. For these materials, when in thin film form, the shape anisotropy dictates that the magnetization lies in-plane. Therefore, for values of θ that are not equal to 90°, the magnetization is not generally co-linear to the applied field and is instead described by the polar angle ψ. For a given ω, sweeping the applied field at a fixed θ yields a more general version of the Kittel equation which describes the field-frequency relationship for FMR:[32]

$$\omega_0^2 = \gamma H^2 + 4\pi M_{eff} H(\sin\theta\sin\psi - 2\cos\theta\cos\psi) + (4\pi M_{eff})^2\cos^2\psi. \quad (1)$$

Here, γ is the gyromagnetic ratio and M_{eff} is the effective saturation magnetization of the FM layer. We note that the above expression reduces to the well-known expression for FMR in a thin film when $\theta = 90°$: $\omega_0 = \gamma\sqrt{H(H + 4\pi M_{eff})}$.

It is common in ST-FMR experiments for the magnetization of the FM layer to be treated as a single large "macrospin". Under this macrospin approximation, the following equation of motion can be used to describe the macrospin under the influence of FL and DL torques:[1]

$$\frac{d\hat{\mathbf{m}}}{dt} = -\gamma\hat{\mathbf{m}} \times \mathbf{H} + \alpha\hat{\mathbf{m}} \times \frac{d\hat{\mathbf{m}}}{dt} + \gamma\tau_F\hat{\mathbf{m}} \times \hat{y} + \gamma\tau_D\hat{\mathbf{m}} \times (\hat{y} \times \hat{\mathbf{m}}). \tag{2}$$

Here, α is the magnetic damping parameter, τ_D is the DL driving torque, and τ_F is the FL driving torque. It is implied in the equation of motion that τ_D and τ_F are torque amplitudes that oscillate at the frequency of the signal generator, ω. The directions of the FL torque and the DL torque are determined by the device design, and for the example considered in Figure 1 (a), the field generated by the rf current and the spin polarization of the spin Hall effect are both in the $\hat{y}$-direction.

As indicated in Figure 1 (a), a dc voltage is measured across the sample using a bias-tee at the FMR condition. The dc voltage arises from a rectification mechanism where oscillating anisotropic magnetoresistance[33] (AMR) of the FM layer mixes with the rf current passing through the FM layer.[2] The amplitude of the voltage is proportional to the amplitude of the AMR change from magnetization precession, δR, which can be defined as:

$$\delta R = \frac{\partial R}{\partial \phi}\delta\phi + \frac{\partial R}{\partial \psi}\delta\psi. \tag{3}$$

The magnetization oscillates about a static equilibrium position[32] that is described by (ϕ, ψ) with angular amplitudes, $\delta\phi$ and $\delta\psi$. In ST-FMR experiments these amplitudes are further related to the amplitudes of magnetization precession from solving the equation of motion such that $\delta\phi = m_{x'}$ and $\delta\psi = m_{z'}$.[1] In Figure 1 (d) we illustrate the dynamic amplitudes, $m_{x'}$ and $m_{z'}$, that are obtained from solving the linearized equation of motion in a rotated coordinate system where the magnetization lies along the y' direction. We also denote a phase angle, β, which is related to phase difference between the rf current passing through the sample, and the magnetization precession. Assuming that the rf signal passing through the NM/FM bilayer is a cosine function, β is the phase of the precession at t = 0. The dc voltage that develops across the sample near and on resonance is then given as $V_{dc} = \frac{1}{2} I_{rf} \delta R$, where I_{rf} is the rf current amplitude through the FM layer.

By solving the equation of motion, it can be shown that the lineshape of the dc voltage is described by the following function:[1]

$$V_{dc} = \frac{S\Delta + A(\omega^2 - \omega_0^2)}{(\omega^2 - \omega_0^2)^2 + \Delta^2}. \tag{4}$$

The lineshape is a superposition of a symmetric term, with amplitude S, and an antisymmetric term, with amplitude A. A linewidth parameter, Δ, is usually a fitting parameter. The amplitudes S and A have a non-trivial angular dependence that depend on the FL and DL torques:

$$S = \frac{1}{2} I_{rf}[\frac{\partial R}{\partial \phi}\omega\gamma(\tau_D \cos\phi - \tau_F \cos\psi \sin\phi) - \sin\psi \frac{\partial R}{\partial \psi}\omega\gamma(\tau_D \cos\psi \sin\phi + \tau_F \cos\phi)] \tag{5}$$

$$A = \frac{1}{2} I_{rf}[\frac{\partial R}{\partial \phi}\gamma^2(\tau_D \cos\psi \sin\phi + \tau_F \cos\phi) \times (H_0 \cos(\theta - \psi) - 4\pi M_{eff} \cos 2\psi) - \sin\psi \frac{\partial R}{\partial \psi}\gamma^2(\tau_D \cos\phi - \tau_F \sin\phi \cos\psi)(H_0 \cos(\theta - \psi) - 4\pi M_{eff} \cos\psi^2)] \tag{6}$$

For any value of θ and ψ not equal to 90°, the amplitudes S and A are not invariant under field/magnetization reversal. We define magnetization and field reversal by $\theta \to 180° - \theta$, $\psi \to 180° - \psi$ and $\phi \to \phi + 180°$. The field/magnetization reversal asymmetries in the amplitudes of S and A are a direct consequence of the unidirectional dynamic effect, and originate from asymmetries in the amplitudes $m_{x'}$, $m_{z'}$, and β found from solving the equation of motion. In other words, the lineshape asymmetry arises because the magnetization precession amplitudes and phase are not invariant under field/magnetization reversal.

Perhaps the most intriguing aspect of the unidirectional dynamics is that when the magnetization is tipped out of the sample's plane, the dynamic amplitudes can be more efficiently exited in one orientation as compared to the field-reversed counterpart. Before beginning an extended illustration of this effect we state that for the duration of the manuscript we will be utilizing the phenomenological model described above under the assumption that the material is permalloy and that the ST-FMR is driven at a fixed frequency of 5.5 GHz. We will be describing how, under these assumptions, the unidirectional dynamics manifest, and what the implications on the measured ST-FMR signal are. In Figure 2 (a) and (b) we plot trajectories which represent the magnitude of the dynamic amplitudes, $m_{x'}$ and $m_{z'}$, as the field is rotated out-of-plane. Every point along the trajectory represents the FMR configuration for a driving frequency of 5.5 GHz for differing polar angle configurations. In (a), we examine the '+' configuration where $\phi = 45°$ and $0° < (\theta, \psi) < 90°$. Every trajectory starts on the dashed line, which represents the in-plane orientation, and ends at the point which represents the out-of-plane orientation (where all trajectories meet). The heavy red trajectory represents a pure FL torque driving the dynamics, and the heavy blue trajectory represents a pure DL torque. As the color bar indicates, colors on the spectrum between red and blue represent different torque mixtures. It is clear that by adding a DL component to a pure FL torque or adding a FL component to a pure DL torque, the magnitudes of $m_{x'}$ and $m_{z'}$ tend to increase. In other words, for the '+' configuration the dynamics are enhanced. In (b) we examine the field reversed, '-' configuration where $\phi = 225°$ and $90° < (\theta, \psi) < 180°$. The color scale is the same in (a) and (b), and it is also clear that the heavy red and heavy blue lines, representing the pure FL and DL torque cases, are identical between (a) and (b). This is a reflection of the fact that there is no unidirectional effect for pure FL and DL torques.[1] However, in (b), we see that in the '-' configuration, adding a DL component to a FL torque (or vice versa) actually suppresses the dynamic amplitudes; this is in contrast to (a) where dynamics are enhanced.

In Figure 2 (c), we further illustrate the unidirectional dynamics by plotting the elliptical precession of the magnetization dynamics driven by a pure FL torque, a pure DL torque, and an equal combination of FL and DL torques. Although the torque composition varies, we keep the magnitude of the combination of τ_F andτ_D normalized. These orbits are calculated at the FMR field, assuming a signal of 5.5 GHz, and are obtained at angular coordinates of $(\phi, \theta, \psi) = (45°, 8°, 75°)$ which we call the '+' orientation. The trajectories are also calculated for the field-reversed orientation where $(\phi, \theta, \psi) = (225°, 172°, 105°)$, which we call the '-' orientation. If the magnetization is driven by a pure FL torque (red trajectory) or a pure DL torque (blue trajectory), the trajectory is found to be invariant under field/magnetization reversal. If the magnetization is driven by an equal combination of FL and DL torques, as indicated by the purple trajectories, the trajectories are no longer invariant. The filled purple circles represent the '+' orientation, which is driven more efficiently than the '-' orientation represented by open purple circles.

In addition to the dynamic amplitudes, $m_{z'}$ and $m_{x'}$, we have illustrated a phase angle, β, in Figure 1 (d) that describes the phase of precession relative to the oscillating current which passes through the device. Generally speaking, this angle is important in determining the shape of the ST-FMR lineshape which is experimentally measured. For the simple in-plane magnetized situation, if $\beta = 90°$, the lineshape is completely antisymmetric (when driven by just a FL torque), and if $\beta = 0°$ the lineshape is completely symmetric (when driven by just a DL torque). When the magnetization is driven by a linear combination of a FL and DL torque, β can be set to any arbitrary angle depending on the relative strength between the FL and DL torque. In the context of unidirectional dynamics, as the magnetization is tipped out-of-plane, when both a FL and DL torque drives the dynamics, β has an asymmetric response under field/magnetization reversal. In Figure 2 (d) we plot β as a function of the out-of-plane field angle, θ, where ST-FMR occurs if ω is set to 5.5 GHz. The inset in (b) shows the simple case of a pure FL torque (open and closed blue squares), a pure DL torque (open and closed red squares). Note that the evolution of the phase angle β is mirror symmetric about $\beta = 0°$ as θ is varied when only a pure FL or pure DL is driving the dynamics. When there is a combination of a FL and DL torque driving the dynamics no such symmetry exists. We plot the evolution of β for the case where an equal strength, FL and DL torques are driving the dynamics. Closed purple circles represent the '+' configuration while open purple circles represent the '-' configuration. It is clear that the phase evolution of β is highly asymmetric under field/magnetization reversal as the field/magnetization is tipped out of the sample's plane.

3. DISCRIMINATING PHASE SHIFTS FROM DAMPING-LIKE TORQUES

We are now poised to outline how one can exploit unidirectional magnetization dynamics to help resolve an issue previously identified by Harder *et al.*, where for some samples and device geometries, appreciable phase shifts can occur between the rf current passing through the device and the FL torque.[31] We propose a method to detect and further quantify these non-zero phase shift effects.

Suppose that there is a non-zero phase shift, δ, between the FL torque and the rf current. Assuming that there is no DL torque present, the lineshape amplitudes, S and A, have the following form:

$$S = a_1 \sin\delta + a_2 \cos\delta, \tag{7}$$

$$A = a_1 \cos\delta - a_2 \sin\delta, \tag{8}$$

$$a_1 = \frac{1}{2} I_{rf}[\frac{\partial R}{\partial \phi}\gamma^2(\tau_F \cos\phi) \times (H_0 \cos(\theta-\psi) - 4\pi M_{eff}\cos 2\psi) + \sin\psi \frac{\partial R}{\partial \psi}\gamma^2(\tau_F \sin\phi\cos\psi)(H_0\cos(\theta-\psi) - 4\pi M_{eff}\cos\psi^2)], \tag{9}$$

$$a_2 = \frac{1}{2} I_{rf}[-\frac{\partial R}{\partial \phi}\omega\gamma(\tau_F \cos\psi \sin\phi) - \sin\psi \frac{\partial R}{\partial \psi}\omega\gamma(\tau_F\cos\phi)]. \tag{10}$$

The above equations imply that one measures a non-zero S and A for a FL torque which is phase shifted, even in the absence of a DL torque. What makes matters worse is that the experimenter cannot simply perform the typical, in-plane, ϕ-dependent angular characterization to distinguish a phase-shifted FL torque from a FL and DL torque pair. In other words, a FL torque strongly phase shifted from the rf current can lead to large amplitudes for S and A, with the same in-plane angular dependence; this is exactly the same result one measures if both a FL and DL torque are present.[1] However, by exploiting the unidirectional dynamic effect, and carrying out a θ-dependent angular characterization of the ST-FMR lineshape, it can be verified that values of S and A arise from a DL and FL torque combination as opposed to a phase-shifted FL torque.

Consider an example where a ST-FMR signal is measured to have an amplitude ratio of $S/A = 1$ when the field is applied in-plane. The amplitude ratio of $S/A = 1$ can occur if the FL-torque is out-of-phase with the rf-current such that $\delta = 45^\circ$ and $\tau_D = 0$. Alternatively, the same ratio can occur if $\delta = 0$ and $\tau_F/\tau_D = .2045$. The lineshape for these two cases is shown in Figure 3 (a), where four lineshapes are plotted for $\phi = 45^\circ$ and $\theta, \psi = 90^\circ$ and the field-reversed angular counterpart. Note that although four cases are considered, there are only two lineshapes because the phase shifted FL torque lineshape is indistinguishable from the FL and DL torque pair. Next, we fix $\phi = 45^\circ$ and explore the angular dependence of S/A as a function of ψ. In Figure 3 (b) we illustrate this effect by showing our model's prediction of the lineshapes when $\phi = 45^\circ$ and $\theta = 27^\circ$ and also for the field reversed case when $\phi = 225^\circ$ and $\theta = 153^\circ$. In (b) we can clearly differentiate between the two cases as evidenced by the four distinct lineshapes. In Figure 3 (c), we plot the amplitudes ratio S/A as a function of θ for $\phi = 45^\circ$. It is clear that as the field is tipped out-of-plane, leading to enhanced unidirectional effects, the four trajectories of S/A significantly separate leading to a clear identification of a phase-shifted FL torque from a FL and DL torque pair.

4. CONCLUSION AND OUTLOOK

In this work we have reviewed the phenomenology behind a recent result where we have discovered that spin-torque driven magnetization dynamics has a directional preference if a field-like torque is present as well.[1] We then examined how in addition to the precession amplitudes, the starting phase angle of the magnetization dynamics has a directional

asymmetry. This collection of asymmetries only becomes prominent when the magnetization is tipped out of the plane of the sample. This trait, of how the asymmetries evolve, is a unique signature of the unidirectional dynamics, and it is not shared by a situation where only a field-like torque drives the magnetization dynamics. This is important because when ST-FMR experiments only are performed with magnetization and magnetic fields in the sample plane, in principle, one cannot distinguish a phase-shifted field-like torque from a combination of damping- and field-like torques driving the dynamics. Consequently, we demonstrate that by tipping the magnetization out-of-plane the unidirectional dynamic effect can be used to distinguish these two scenarios from one another. Thus, by simply performing ST-FMR measurements in orientations where the magnetization is oblique to the sample's plane, we have devised a more stringent test that can be performed on new materials exhibiting damping-like torques that have an unknown origin and are currently called into question.

Work at the University of Illinois at Urbana-Champaign, including manuscript preparation, was supported by the National Science Foundation MRSEC program under NSF award number DMR-1720633. Work at Argonne, including theoretical analysis and discussion, was supported by The U.S. Department of Energy, Office of Science, Materials Science and Engineering Division.

References

[1] J. Sklenar, W. Zhang, M. B. Jungfleisch, H. Saglam, S. Grudichak, W. Jiang, J. E. Pearson, J. B. Ketterson and A. Hoffmann, Phys. Rev. B, **95**, 224431 (2017).

[2] L. Liu, T. Moriyama, D. C. Ralph and R. A. Buhrman, Phys. Rev. Lett. **106**, 036601 (2011).

[3] A. Hoffmann, IEEE Trans. Magn. **49**, 5172 (2013).

[4] W. Zhang, W. Han, X. Jian, S. -H. Yang and S. S. P. Parkin, Nature Phys. **11**, 496-502 (2015).

[5] L. Liu, C. -F. Pai, Y. Li, H. W. Tseng, D. C. Ralph and R. A. Buhrman, Science **336**, 555 (2012).

[6] C. -F. Pai, L. Liu, Y. Li, H. W. Tseng, D. C. Ralph and R. A. Buhrman, Appl. Phys. Lett. **101**, 122404 (2012).

[7] C. He, A. Navabi, Q. Shao, G. Yu, D. Wu, W. Zhu, C. Zheng, Z. Li, Q. L. He, S. A. Razavi, K. L. Wong, Z. Zhang, P. K. Amirri and K. L. Wang, Appl. Phys. Lett. **109**, 202404 (2016).

[8] W. Zhang, M. B. Jungfleisch, F. Freimuth, W. Jiang, J. Sklenar, J. E. Pearson, J. B. Ketterson, Y. Mokrousov and A. Hoffmann, Phys. Rev. B **92**, 144405 (2015).

[9] J. Sklenar, W. Zhang, M. B. Jungfleisch, W. Jiang, H. Saglam, J. E. Pearson, J. B. Ketterson and A. Hoffmann, AIP Advance **6**, 055603 (2016).

[10] H. Saglam, J. C. Rojas-Sanchez, S. Petit, M. Hehn, W. Zhang, J. E. Pearson, S. Mangin, and A. Hoffmann, arxiv:1804.01612.

[11] A. R. Mellnik, J. S. Lee, A. Richardella, J. L. Grab, P. J. Mintun, M. H. Fischer, A. Vaezi, A. Manchon, E. -A. Kim, N. Samarth and D. C. Ralph, Nature **511**, 449 (2014).

[12] M. B. Jungfleisch, W. Zhang, J. Sklenar, W. Jiang, J. E. Pearson, J. B. Ketterson and A. Hoffmann, Phys. Rev. B **93**, 224419 (2016).

[13] W. Zhang, J. Sklenar, B. Hsu, W. Jiang, M. B. Jungfleisch, K. Sarkar, F. Y. Fradin, Y. Liu, J. E. Pearson, J. B. Ketterson, Z. Yang and A. Hoffmann, APL Mater. **4**, 032302 (2016).

[14] D. MacNeill, G. M. Stiehl, M. H. D. Guimarães, R. A. Buhrman, J. Park, and D. C. Ralph, Nature Phys. **13**, 300-305 (2017).

[15] D. MacNeill, G. M. Stiehl, M. H. D. Guimarães, N. D. Reynolds, R. A. Buhrman and D. C. Ralph, Phys. Rev. B **96**, 054450 (2017).

[16] T. Chiba, G. E. W. Bauer and S. Takahashi, Phys. Rev. Applied **2**, 034003 (2014).

[17] T. Chiba, M. Schreier, G. E. W. Bauer, and S. Takahashi, J. Appl. Phys. **117**, 17C715 (2015).

[18] M. Schreier, T. Chiba, A. Niedermayr, J. Lotze, H. Huebl, S. Geprägs, S. Takahashi, G. E. W. Bauer, R. Gross and S. T. B. Goennenwein, Phys. Rev. B **92**, 144411 (2015).

[19] J. Sklenar, W. Zhang, M. B. Jungfleisch, W. Jiang, H. Chang, J. E. Pearson, M. Wu, J. B. Ketterson and A. Hoffmann, Phys. Rev. B **92**, 174406 (2015).

[20] M. B. Jungfleisch, W. Zhang, J. Sklenar, J. Ding, W. Jiang, H. Chang, F. Y. Fradin, J. E. Pearson, J. B. Ketterson, V. Novosad, M. Wu and A. Hoffmann, Phys. Rev. Lett. **116**, 057601 (2016).

[21] M. B. Jungfleisch, J. Ding, W. Zhang, W. Jiang, J. E. Pearson, V. Novosad and A. Hoffmann, Nano Lett. **17**, 8-14 (2017).

[22] Z. Fang, A. Mitra, A. L. Westerman, M. Ali, C. Ciccarelli, O. Cespedes, B. J. Hickey and A. J. Ferguson, Appl. Phys. Lett. **110**, 092403 (2017).

[23] M. B. Jungfleisch, J. Sklenar, J. Ding, J. Park, J. E. Pearson, V. Novosad, P. Schiffer and A. Hoffmann, Phys. Rev. Applied **8**, 064026 (2017).

[24] C. O. Avci, K. Garello, A. Ghosh, M. Gabureac, S. F. Alvarado and P. Gambardella, Nat. Phys. **11**, 570-575 (2015).

[25] S. S. -L. Zhang and G. Vignale, Phys. Rev. B. **94**, 140411(R) (2016).

[26] S. Langenfeld, V. Tshitoyan, Z. Fang, A. Wells, T. A. Moore and A. J. Ferguson, Appl. Phys. Lett. **108**, 192402 (2016).

[27] K. J. Kim, T. Moriyama, T. Koyama, D. Chiba, S. W. Lee, S. J. Lee, K. J. Lee, H. W. Lee and T. Ono, arXiv:1603.08746.

[28] K. Yasuda, A. Tsukazaki, R. Yoshimi, K. S. Takahashi, M. Kawasaki and Y. Tokura, Phys. Rev. Lett. **117**, 127202 (2016).

[29] H. T. Nembach, J. M. Shaw, M. Weiler, E. Jué and T. J. Silva, Nat. Phys. **11**, 825-829 (2015).

[30] K. Di, V. L. Zhang, H. S. Lim, S. C. Ng, M. H. Kuok, J. Yu, J. Yoon, X. Qiu and H. Yang, Phys. Rev. Lett. **114**, 047201 (2015).

[31] M. Harder, Z. X. Cao, Y. S. Gui, X. L. Fan, and C.-M. Hu, Phys. Rev. B **84**, 054423 (2011).

[32] S. Lee, S. Grudichak, J. Sklenar, C. C. Tsai, M. Jang, Q. Yang, H. Zhang, and J. B. Ketterson, J. App. Phy. **120**, 033905 (2016).

[33] T. R. McGuire amd R. I. Potter, IEEE Trans. Magn. **11**, 1018 (1975).

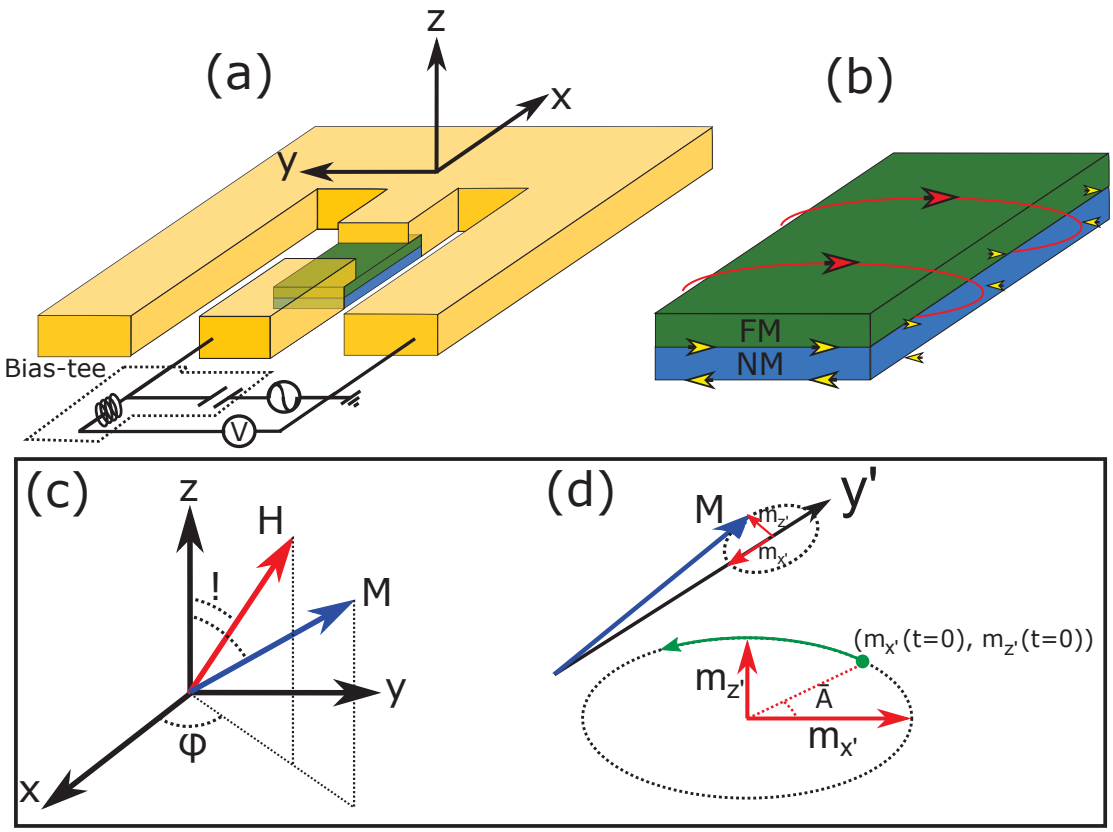

Figure 1: (a) a schematic drawing of a NM/FM bilayer (blue and green slabs) integrated into a co-planar waveguide geometry (golden stripline). The circuit drawing illustrates that by using a bias-tee (dashed line), a high frequency signal generator can transmit an rf-current through the bilayer while the dc voltage across the bilayer is monitored. (b) illustrates how in the NM/FM bilayer, a magnetic field can be generated from the NM layer onto the FM layer (red arrows). Additionally, we assume that the NM layer has a spin Hall effect, where a spin current flows from the NM layer into the FM layer, thereby causing a STT. The polarization of the spin current is illustrated by the yellow arrows. (c) is the coordinate system we will refer to; note that due to the thin film geometry, the magnetization and field are not generally co-linear. (d) illustrates a coordinate system where the y'-direction is rotated to align along the magnetization direction. In this coordinate scheme the magnetization precession can be descibred by two dynamic amplitude $m_{x'}$, $m_{z'}$ and a phase angle β.

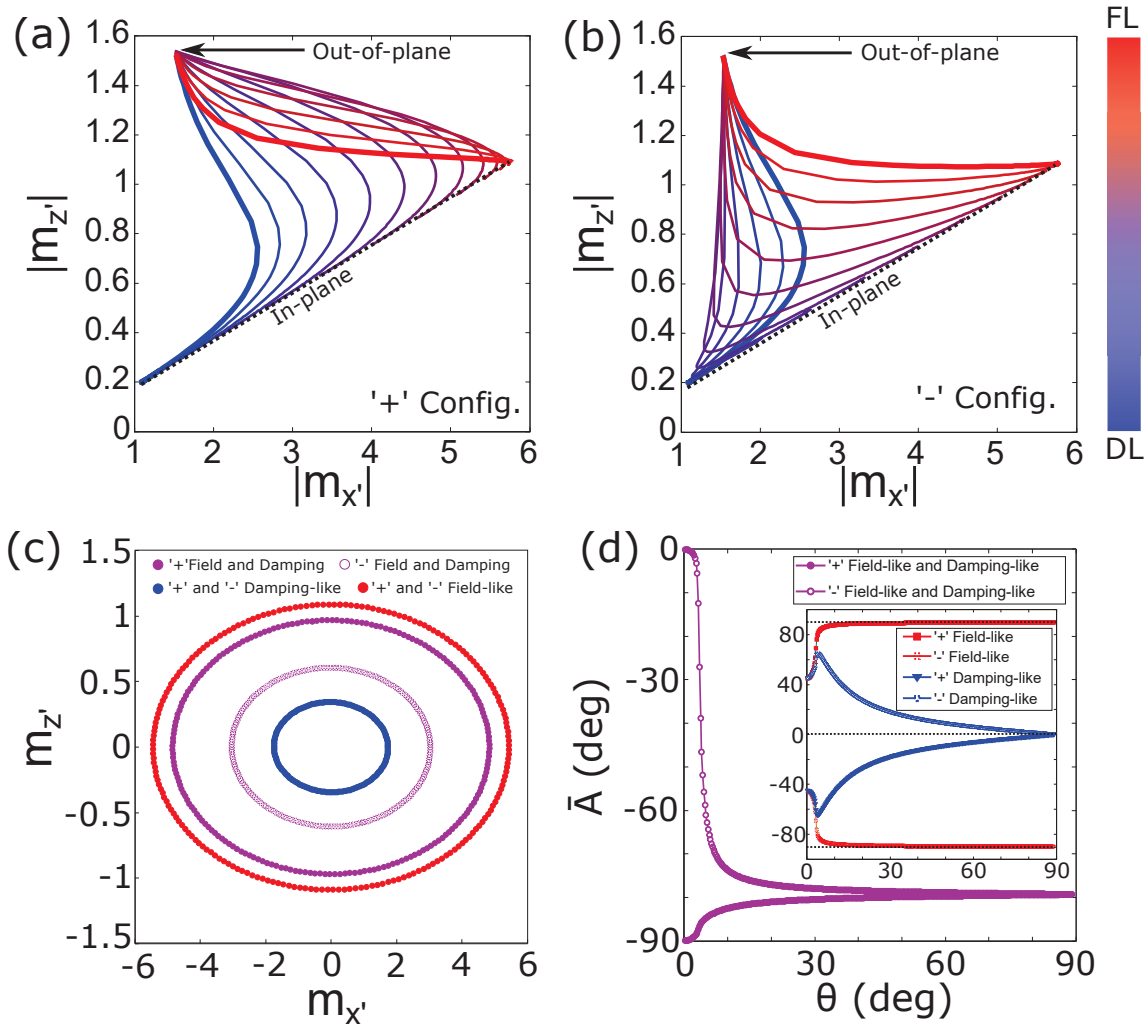

Figure 2: (a) and (b) are trajectories of the dynamic amplitudes $m_{x'}$ and $m_{z'}$ for various FL and DL torque combinations. The trajectories begin along a dashed line which represents when the magnetization lies in-plane. The trajectories end at a point which represents when the magnetization lies out-of-plane. In (a), the '+' magnetization configuration defined in text is used, and (b) is the '-' configuration representing the field/magnetization reversal state of '+'. For any case where both a FL and DL torque are both present, the trajectories are not invariant between the '+' and '-' configuration. In (c) we plot the elliptical precession orbits for an instance of the '+' configuration (ϕ, θ, ψ) = (45°, 8°, 75°) and an instance of the '-' configuration where (ϕ, θ, ψ) = (225°, 172°, 105°). For pure FL and DL torques, the orbits are invariant between the '+' and '-' configuration, but they are asymmetric when a FL and DL torque are present with equal magnitudes. In (d) we plot how the phase angle, β, varies as a function of the field polar angle, θ. In the main portion of (d), closed circles represent the '+' configuration and open circles represent the '-' configuration when both a FL and DL torque are present. Here, there is no obvious symmetry in how β changes between the '+' and '-' configuration. The inset shows a pure DL torque in blue and a pure FL torque in red. For both of these cases when a single torque is driving the dynamics, when the field/magnetization is reversed, β goes to $-\beta$.

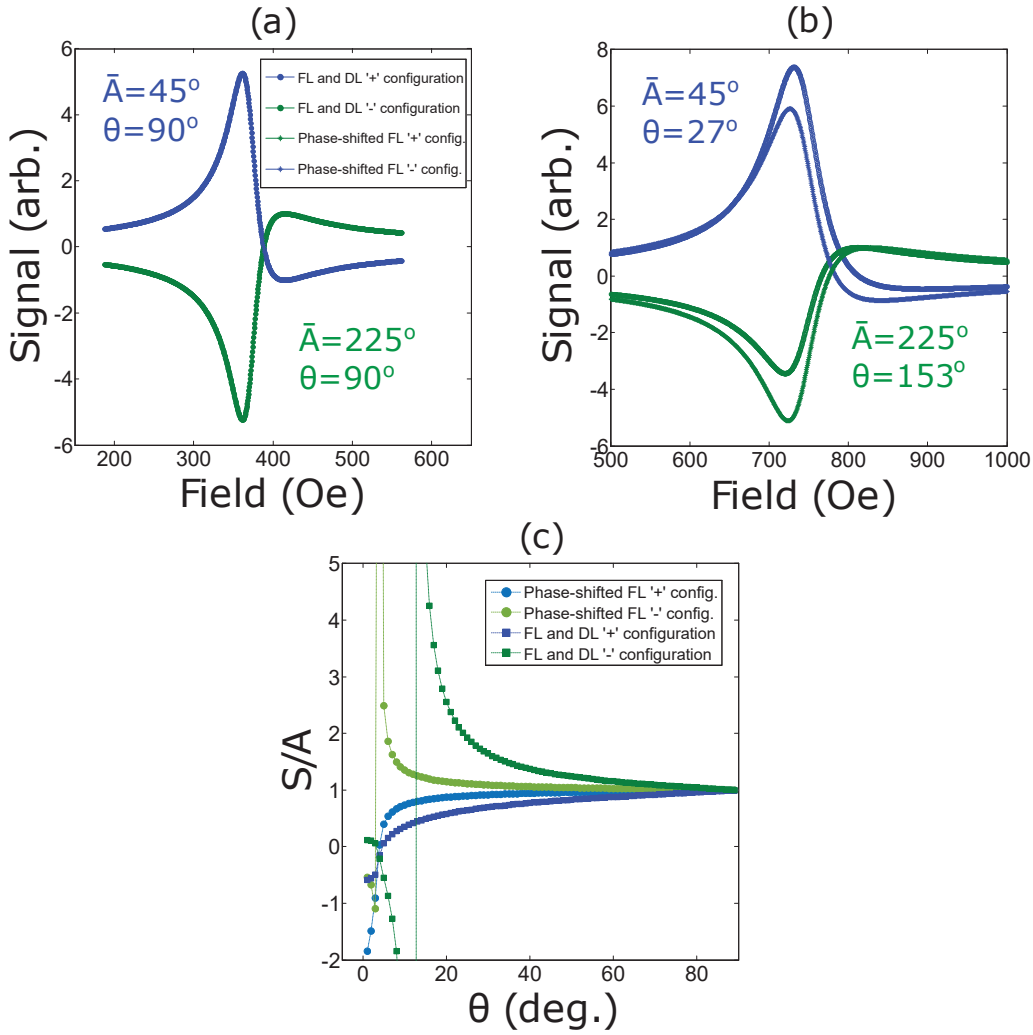

Figure 3: (a) we show how the ST-FMR lineshape is indistinguishable in a case when a FL torque is phase shifted from the rf-current compared to a case where both a FL and DL torque are present. The lineshapes are generated from the phenomenological model presented in the text, and the angular configuration in (a) represents a situation where the magnetization lies in-plane and is driven to resonance at 5.5 GHz. In (b) we demonstrate how when the field is tipped out-of-plane, a phase-shifted FL torque and a FL and DL torque pair cause the lineshape to evolve in different ways. Consequently, the two cases are now distinguishable. In (c) we plot the symmetric lineshape amplitude S divided by the antisymmetric amplitude A as a function of θ. The ratio of S/A is the same for both '+' and '-' configurations when the field is in-plane for both scenarios, but as the field is rotated out-of-plane each trajectory evolves differently. We note that the driving frequency is held fixed at 5.5 GHz for this entire demonstration. This result illustrates how the out-of-plane angular dependence of the ST-FMR signal can be used to distinguish phase-shifted FL torques from FL and DL torque pairs.